JP1.5 DIURNAL RELATIONSHIPS BETWEEN SOIL HEAT FLUX AND NET RADIATION OVER A RANGE OF SURFACE CONDITIONS APPLIED TO LAND SURFACE ENERGY BALANCE MODELING

Joseph A. Santanello, Jr.* and Mark A. Friedl
Department of Geography, Boston University

1. Introduction

Because soil heat flux (G) is typically the energy balance's smallest term, it is often estimated as a constant function of net radiation (R_n) (Brutsaert, 1982), as a residual term of the energy balance equation, or assumed to be negligible on daily time scales (Kustas *et al.*, 1993). Traditional approaches to estimating soil heat flux (G) in land surface energy balance models fit regression relationships to measurements of G and R_n to derive a constant, c (where $G = cR_n$), that is fixed for the entire day or period of interest. Such simple treatments enable energy balance closure with minimal demand for specific site information and computation.

However, empirical studies have shown that G is neither constant nor negligible on diurnal time scales, and can constitute as much as 50% of R_n under sparse canopy and bare soil conditions (Clothier *et al.*, 1986). Field observations show that G/R_n can range from 0.05 to 0.50, and is dependent on the time of day, soil moisture and thermal properties, and vegetation amount and height (Kustas *et al.*, 1993). Fuchs and Hadas (1972) and Idso *et al.* (1975) and others have confirmed that for bare and sparsely-covered soils, G/R_n is maximum in mid-morning, and decreases to zero by late afternoon.

With these issues in mind, the purpose of this work is to apply empirical data and results from past experiments combined with simulations by a multi-layer, diffusion-based soil model to develop robust relationships between G/R_n and time of day, surface conditions, and vegetation cover. In doing so, these relationships will more accurately describe the proportion of net radiation that goes into soil heat flux relative to current simplified but widely used approaches, and by extension improve estimation of LE and H regardless of the type of land surface energy balance (LSEB) closure used.

2. Physical Controls on G/R_n

2.1 Hysteresis in G

Previous studies have noted a distinct diurnal pattern in G/R_n, with well-defined asymmetry about solar noon. Observations confirm that for bare and sparsely-covered soils, G/R_n is maximum in mid-morning, and decreases to zero by late afternoon. Ignoring this asymmetry can underestimate G in the morning and overestimate G in the afternoon by up to 50%, resulting in corresponding errors in the turbulent flux terms of the LSEB.

*Corresponding author address: Joseph A. Santanello, Jr., Boston University, Dept. of Geography, Boston, MA, 02215; e-mail: sntnello@crsa.bu.edu

2.2 Soil Moisture

Field work has shown significant variation in maximum daily values of G/R_n, ranging from 0.05 - 0.50, depending on the degree of soil wetness and the canopy cover.

2.3 Vegetation Density

For a full canopy G/R_n is generally less than 0.10 with little diurnal variation, in which case a constant midday value works reasonably well. However, values for sparse canopies and bare soil can range from 0.20 to 0.50 and retain a distinct diurnal trend.

3. Model and Site Description

The Simultaneous Heat and Water (SHAW; Flerchinger *et al.* 1998) model is a 1-D, multi-layer soil and vegetation model that simulates the movement of heat and water through canopy, residue, snow, and soil layers. The flexible layering and complex treatment of canopy and soil processes make it desirable for this study. Simulations were performed using data from the Lucky Hills site of the Monsoon '90 field campaign, which provides a reliable dataset over a sparsely (< 25% cover) vegetated region (Kustas and Goodrich, 1994). SHAW was tested successfully over the this site during a dry-down period in July-August. Surface fluxes simulated for 3 cloud-free days (207, 208, 220) are well within acceptable error ranges (~10%).

4. Simulation Results and Parameterizations

Using typical atmospheric and surface conditions for the Lucky Hills site, SHAW simulations were performed varying the soil type and corresponding hydraulic properties, and subsequently varying the initial soil moisture profile from near-saturation (volumetric soil moisture, $\theta = 0.40$) to desiccated conditions ($\theta = 0.05$) for each soil type. The resulting relationships between G/R_n, time of day, soil type, and moisture content were then examined.

4.1 Moist Soils

Figure 1 shows the diurnal pattern of G/R_n simulated by SHAW for 11 soil types, initialized with (near-saturated) conditions (= 0.40) in the upper 2-cm layer

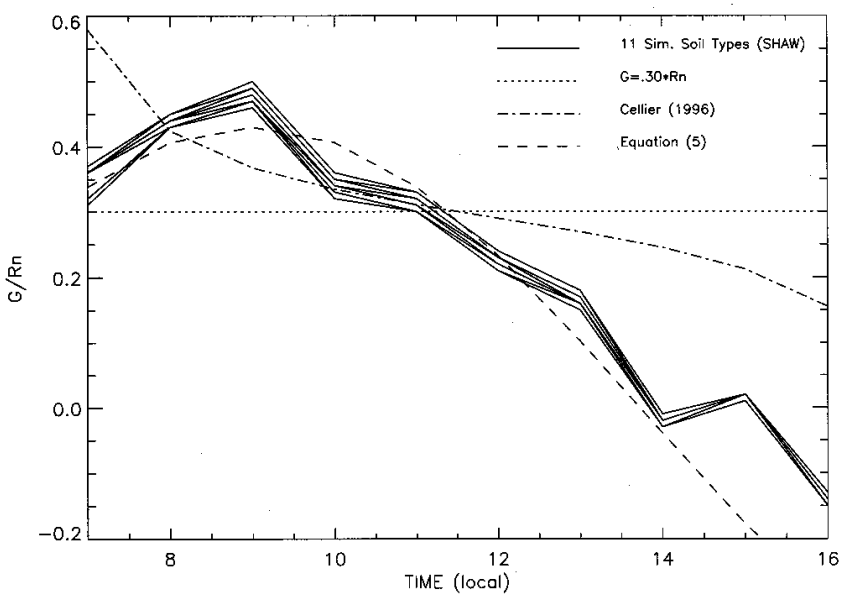

Figure 1. Time series of G/R_n for 11 soil types (Clapp and Hornberger, 1978) using an initial upper volumetric soil moisture of 0.40 and average atmospheric forcing from Monsoon '90. Included are parameterizations from Equation (1), a constant ratio approach, and that of Cellier *et al.* (1996).

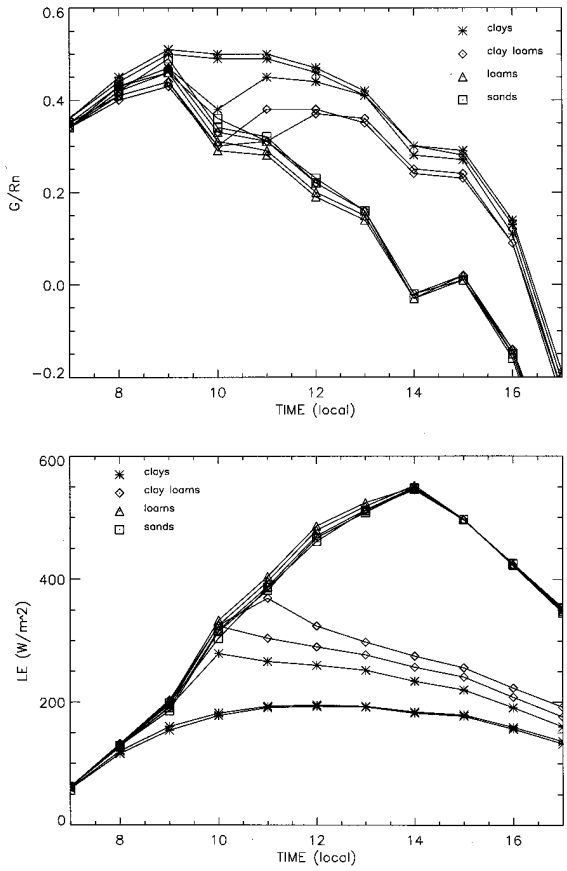

Figure 2. a) Same as for Figure 3, with initial volumetric soil moisture of 0.25. b) Latent heat flux for the period simulated in 4a for the 11 soil types.

(and gradually wetter below). The hysteretic behavior of G/R_n is clear and little variation between soil types is evident. The time of maximum G/R_n is 9 am, 3 hours before the maximum incoming net radiation (Figure 1). These results may be approximated in a straightforward fashion using a function of the form,

$$G/R_n = A*\cos((2p*3600*t)/B) \quad (1)$$

where A represents the maximum value of G/R_n, B is chosen to adjust for the best fit slope of the curve, and t is the time, in hours, before (negative) or after (positive) the maximum. Applying this equation to the data shown in Figure 3 and finding the best fit for the times when G is positive (7 am - 2 pm), yield values of 0.43 and 68,000 s^{-1} for A and B, respectively. The resulting approximation has an RMSE of 0.042 and is plotted in Figure 3 along with a constant G/R_n ratio of 0.30 (RMSE = 0.152), and the phase shift parameterization of Cellier *et al.* (1996) (RMSE = 0.138).

Note that if Equation (1) is to be of practical use, it needs to be relatively insensitive to the choice of constants A and B. Varying A by ±.05 and B by ±10,000 s^{-1} increased the RMSE's only slightly. Thus, there is a substantial margin for error in choosing these values whereby significant improvement over previous methods is still obtained.

4.2 Intermediate Moisture

Diurnal variation in G/R_n for the 11 soil types with initial volumetric soil water content of 0.25 is presented in Figure 4a. Clearly, soil type exerts strong control on the diurnal pattern of G/R_n at intermediate soil moisture levels. In particular, clays and silty clays show substantial rapid drying of the upper soil layers that increases mid- and late-day G/R_n, primarily due to increased available energy to the soil as a result of reduced evaporation.

The best fit of Equation (1) (A = 0.43 and B = 83,000 s^{-1}) to the simulated data in Figure 2 yields an RMSE of .094 versus .137 and .135 for constant ratio and phase shift estimates, respectively. This is again an improvement over earlier methods, and even greater accuracy could be obtained if the soil type and relative soil water content is known for a particular location.

In addition to increasing midday and afternoon G/R_n, stage-2 drying lengthens the period during which G remains positive (downwards) shifts 2 hours later as well. The empirical data of Fuchs & Hadas (1972), Idso *et al.* (1975), Clothier *et al.* (1986), Betts and Ball (1995), and Cellier *et al.* (1996) all generally agree with our simulations.

4.3 Dry Soils

Results from simulations with dry soil conditions (initial soil water content of 0.05), show that relative to more moist conditions, G/R_n is systematically larger, G does not becomes negative until after 4 pm, and evaporation is negligible (not shown). Because well-dried soils are all in stage-2 or stage-3 (desiccated) drying, parameterization of G is more easily implemented independent of soil type. A best fit of Equation (1) to these data has values of 0.49 and 113,000 s^{-1} for A and B, resulting in an RMSE of .061 compared to .184 for a constant ratio (c=0.40) and .095 using a phase shift. Once again, Equation 1 improves estimates of soil heat flux under these conditions even if the soil type information is unknown.

4.4 Influence on LSEB Modeling

(R_n - G) is a measure of the available energy to the surface for evaporation and sensible heating, and is therefore crucial in estimating LSEB. Simulated 'available energy' (R_n - G) using these parameterizations for moist, intermediate, and dry conditions is presented in Table 1, along with (R_n - G) estimated using a constant ratio of 0.30, a 1-hour phase shift, and assuming that G is negligible. Note, that in some cases, the differences in (R_n - G) among the various parameterizations are on the order of 200 Wm^{-2}.

4.5 Vegetation Cover

It is obvious that locations that are densely vegetated do not require such detailed treatment of soil heat flux, which is expectedly low. To examine the sensitivity of (1) to vegetation density, simulations were performed with leaf area index (LAI) assigned values of 0.1, 1.0, 2.5, and 5.0. Results suggest that a single relationship could approximate G/R_n reasonably well for LAI at or above 2.5 for all soil types and water contents and the diurnal pattern in G/R_n remains evident for all vegetation densities. Sparse cover and bare soil, where maximum and overall values of G/R_n reach more than three times those of full cover, do exhibit significant departures as a function of soil type, and would benefit from parameterizations that account for differences in soil type and moisture such as Equation (1). Overall, as vegetation amount increases, the magnitude of soil heat flux decreases rather rapidly as do the confounding influences of soil moisture and soil type.

4.5 Application of Results

The relationships developed and observed here demonstrate the potential improvement in estimating soil heat flux for simple LSEB models, particularly for sparse-cover conditions. Equation (1) captures the diurnal behavior of G/R_n which previous methods lack, and can be adjusted according to soil moisture and texture conditions.

This equation can be used in a semi-empirical manner, as it would require some calibration to determine best use of the constants A and B for each location of interest. A should be chosen relative to the local maximum value of G/R_n, while varying B from 60,000-120,000 s^{-1} from wet to dry soils, with a noticeable shift in the slope seen during the transition from stage-I to stage-II drying. Above an LAI of 3.0, a rather low value (maximum G/R_n) for A and middle range for B would be expected independent of soil

conditions, but should still improve slightly on the constant ratio approach.

To ensure that the results seen here are not model or site-specific, the methodology above was applied to the FIFE site and again compared with other methods of estimating *G*. Without adjusting the fitting parameters and with no knowledge of changes in vegetation or soil conditions, Equation (1) was the best method of parameterizing G/R_n. Using knowledge of the 'green-up' of the FIFE site from June-July, and the drying of the soil from July-August allows adjustment of *A* and *B*, as suggested, to greater improve the accuracy of this method. It is also important to note that this was successful for a completely different region (Kansas) than where the simulations to develop the parameterizations were performed (Arizona).

5. Stages of Soil Drying

The transition to rapid drying of the soil surface occurs when the near-surface soil moisture becomes lower than field capacity, which depends on soil type (Jury *et al*., 1991). Previous studies have quoted thresholds for the transition from stage-1 to stage-2 drying that range from 37-50% of saturation (Capehart and Carlson, 1997), to 49-66% of field capacity (Santanello and Carlson, 2001, van de Griend and Owe, 1994). Regardless of the absolute values of these thresholds, the transition occurs at intermediate soil moisture near 50% of field capacity, and shifts the slope of G/R_n over the course of a day.

A possible application of the results seen here and an improvement to parameterizations of soil heat flux may be found using remote sensing. Specifically, Figures 2a and 2b show that a distinct signal occurs in surface fluxes when the transition to stage-2 drying occurs. As evaporation decreases, the soil surface heats up and both sensible and soil heat fluxes increase as a results of higher surface temperatures. This change in surface skin temperature is detectable from high-resolution satellite data, and therefore might serve as a diagnostic for the transition of G/R_n (and *?E*) from stage-1 to stage-2 drying (Amano and Savlucci, 1999; Salvucci, 1997). For example, the soil surface thermal signal has been used by Friedl (1995) to infer soil surface resistance to evaporation. Using this signal would mitigate some of the requirements for information regarding specific soil type, properties, and moisture characteristics that would improve the parameterization of soil heat flux during different drying stages, for different soils.

6. Conclusions

This work examines the relationships between hourly soil heat flux and net radiation for varying soil conditions, and from these develops a technique to estimate *G* as a function of R_n. The key advantage of this method is that it captures the diurnal behavior of G/R_n over a range of surface conditions, and provides improvement over previous methods of estimating soil heat flux. Although the details and exact tuning depend largely on the soil type and moisture content, capturing hysteresis in G/R_n throughout the day is important for sparse vegetation and bare soil regions. As a result, energy balance simulations that do not utilize multi-layer diffusion models or a great deal of soil information can still be successful and efficient using this simple method.

Acknowledgments. This work was supported by NSF Grant EAR-9725698. Technical assistance with the SHAW model was graciously provided by Gerald Flerchinger. Thanks also to Bill Kustas for providing data, and those involved with the Monsoon '90 project. Climate data and guidance on soil moisture spinups were provided by Guido Salvucci.

Intermediate Soil (θ =0.25)				
Hour	***Eqn. 1***	***Phase Shift***	***G/R_n =.30***	***G = 0***
7	79.67	52.98	88.21	126.01
8	172.62	169.63	206.25	294.64
9	257.54	285.81	316.27	451.82
10	334.69	380.12	399.89	571.27
11	409.68	446.68	453.54	647.91
12	475.38	478.35	471.42	673.46
13	532.71	486.07	465.44	664.91
14	505.43	418.85	388.31	554.73

Table 1. Available Energy (Wm^{-2}) simulated by each parameterization type for moist and dry soil conditions for the hours when *G* is positive.

References

Amano, E., and G. D. Salvucci, 1999: Detection and use of three signatures of soil-limited evaporation. *Remote Sens. Environ.*, **67,** 108-122.

Brutsaert, W., 1982: Evaporation into the atmosphere. D. Reidel Publishing Company, Dordrecht, Holland, 299 pp.

Camuffo, D., and A. Bernardi, 1982: An observational study of heat fluxes and their relationships with net radiation. *Bound. Layer Meteor.*, **23,** 359-368.

Cellier, P., G. Richard, and P. Robin, 1996: Partition of sensible heat fluxes into bare soil and the atmosphere. *Agric. For. Meteor.*, **82,** 245-265.

Clothier, B. E., K. L. Clawson, P. J. Pinter, Jr., M. S. Moran, R. J. Reginato, and R. D. Jackson, 1986: Estimation of soil heat flux from net radiation during the Growth of alfalfa. *Agric. For. Meteor.*, **37,** 319-329.

Cuenca, R. H., M. Ek, and L. Mahrt, 1996: Impact of soil water property parameterization on atmospheric boundary layer simulation. *J. Geophys. Res.*, **101,** 7269-7277.

Flerchinger, G. N., W. P. Kustas, and M. A. Weltz, 1998: Simulating surface energy fluxes and radiometric surface temperatures for two arid vegetation communities using the SHAW model. *J. Appl. Meteorol.*, **37,** 449-460.

Friedl, M.A. 1995: Modeling land surface fluxes using a sparse canopy model and radiometric surface temperature measurements, *Journal of Geophysical Research*, vol. 100, No D12, pp. 25,435-25,446.

Fuchs, M., and A. Hadas, 1972: The heat flux density in a nonhomogeneous bare loessial soil. *Bound. Layer Meteor.*, **3,** 191-200.

Jury, W.A., W.R. Gardner and W.H. Gardner, 1991: Soil Physics (fifth ed.), John Wiley and Sons, New York.

Kustas, W. P., C. S. T. Daughtry, and P. J. Van Oevelen, 1993: Analytical treatment of the relationships between soil heat flux/net radiation ratio and vegetation indices. *Remote Sens. Environ.*, **46,** 319-330.

Kustas, W.P., and D.C. Goodrich, 1994: Preface. *Water Resour. Res.*, **30,** 1211-1225.

Kustas, W. P., X. Zhan, and T. J. Schmugge, 1998: Combining optical and microwave remote sensing for mapping energy fluxes in a semiarid watershed. *Remote Sens. Environ.*, **64,** 116-131.

Kustas, W. P., J. H. Prueger, J. L. Hatfield, K. Ramalingam, and L. E. Hipps, 2000: Variability in soil heat flux from a mesquite dune site. *Agric. For. Meteor.*, **103,** 249-264.

Santanello, J. A., and T. N. Carlson, 2001: Mesoscale simulation of rapid soil drying and its implications for predicting daytime temperature. *J. Hydrometeor.*, **2,** 71-88.

van de Griend, A. A., and M. Owe, 1994: Bare soil surface-resistance to evaporation by vapor diffusion under semiarid conditions. *Water Resour. Res.*, **30,** 181-188.